Hypercrosslinking-Induced Self-Assembled Carbon Nanospheres: Integration of Hollow Structure, Micro-Mesopores, and Nitrogen Doping Synergistic System for Supercapacitors

Qiujin Lang [a], Rui Feng [a] and Buyin Shi[*a]

School of Chemistry and Chemical Engineering, Ning Xia University, Yinchuan 750021, P. R. China

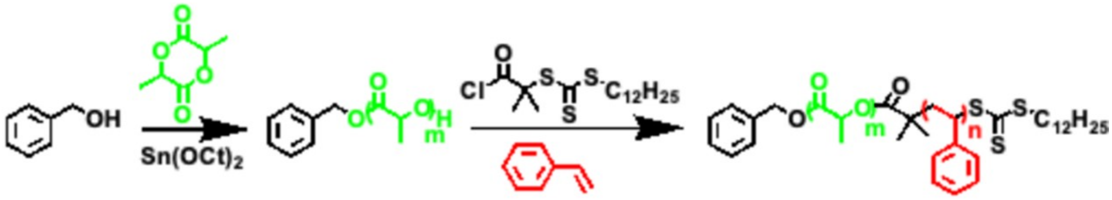

Figure S1. Synthetic route of PLA-b-PS precursor.

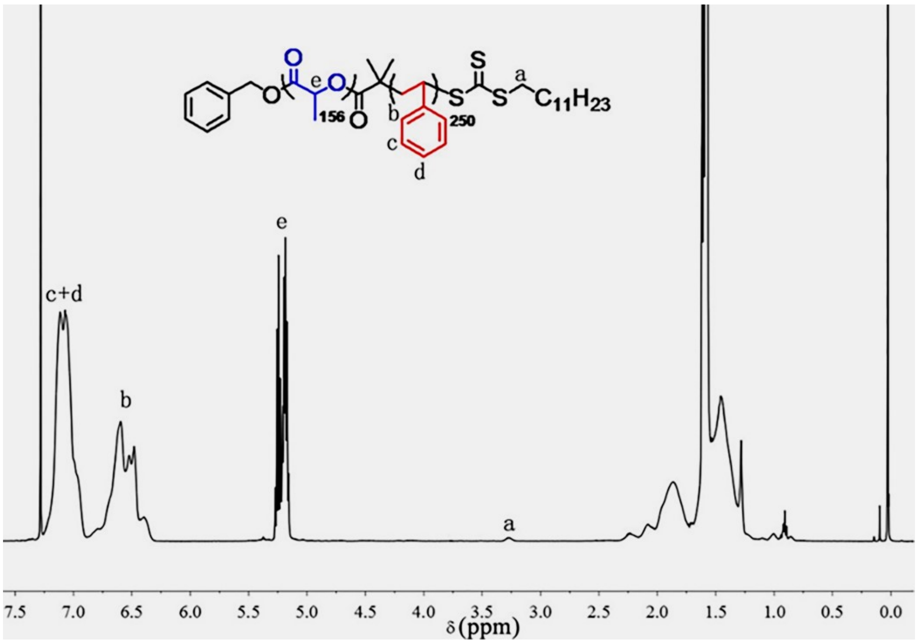

Figure S2. ^{1}H NMR spectrum of PLA_{156}-*b*-PS_{250} diblock copolymer (500 MHz, $CDCl_3$).

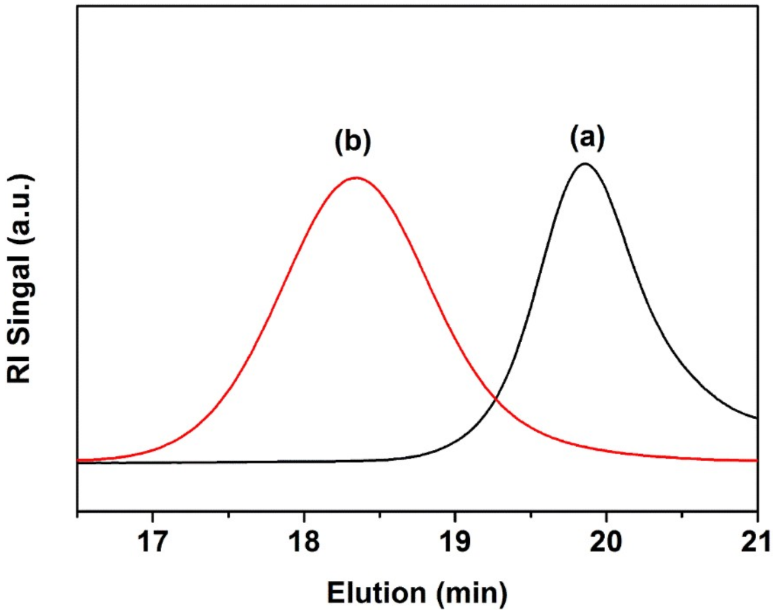

Figure S3. GPC traces of (a) PLA_{70}-b-PS_{100} and (b) PLA_{156}-b-PS_{250} diblock copolymer.

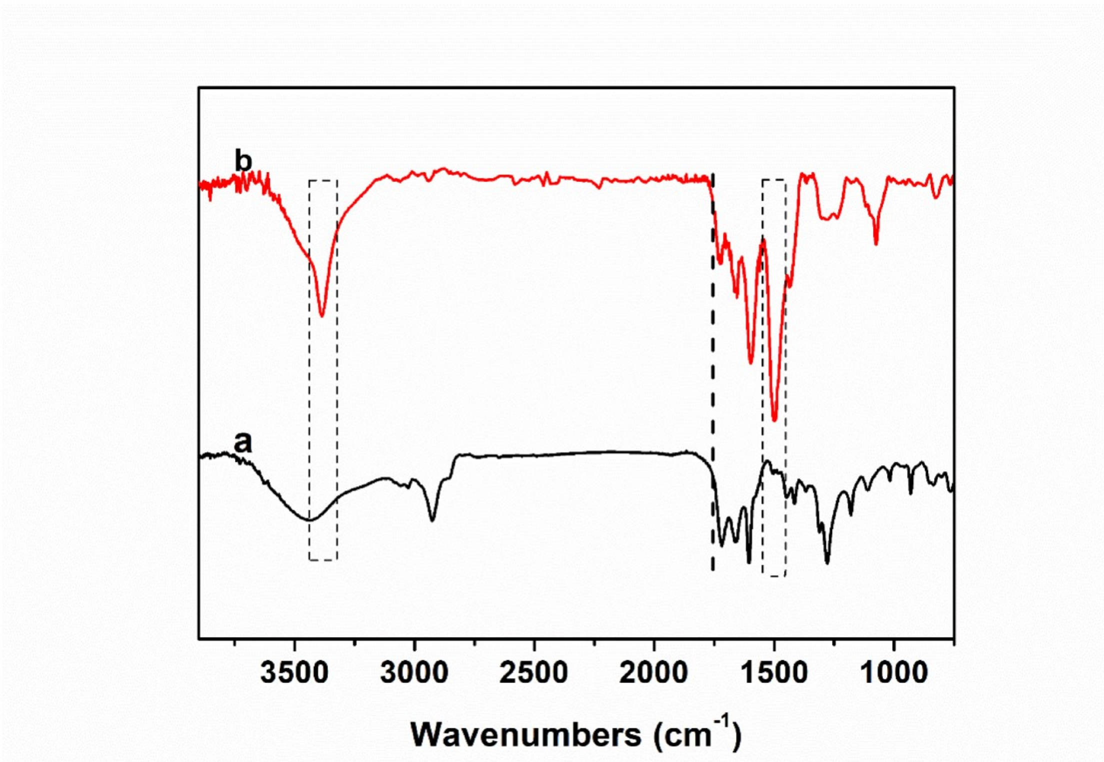

Figure S4. FTIR of (a) hyper-crosslinking PLA_{150}-PS_{250} and (b) PLA_{150}-PS_{250}-N_4.

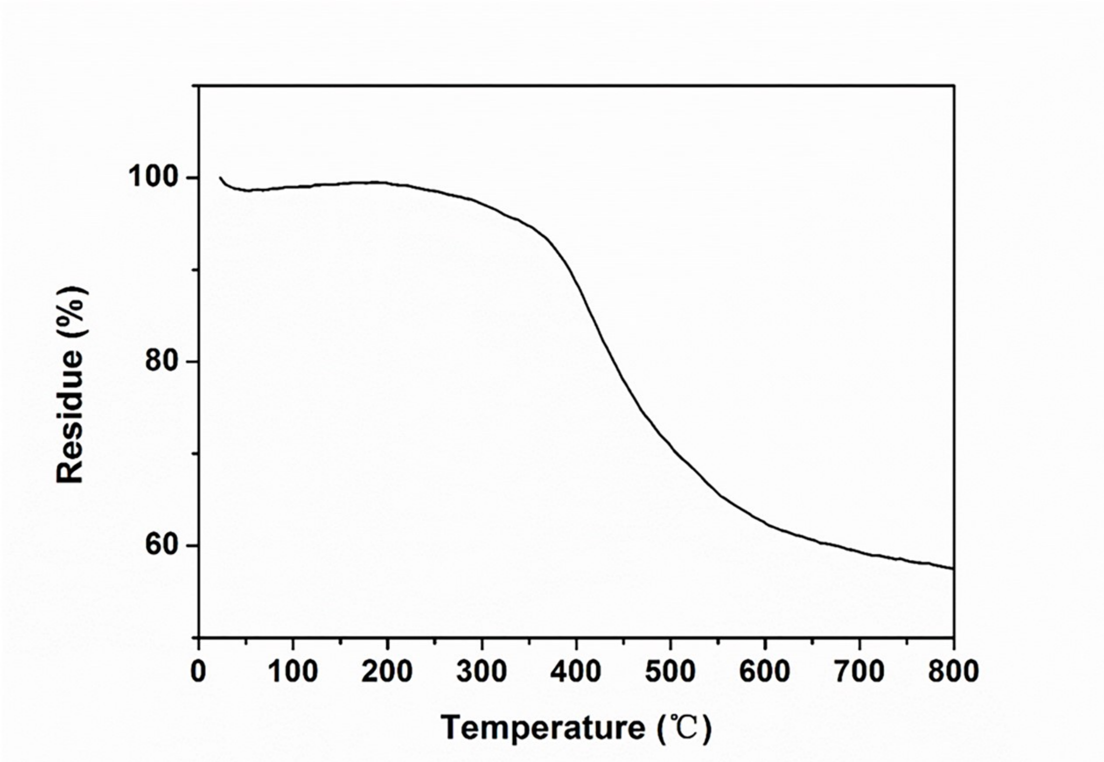

Figure S5. TGA curves of PLA_{150}-PS_{250}-N_4.

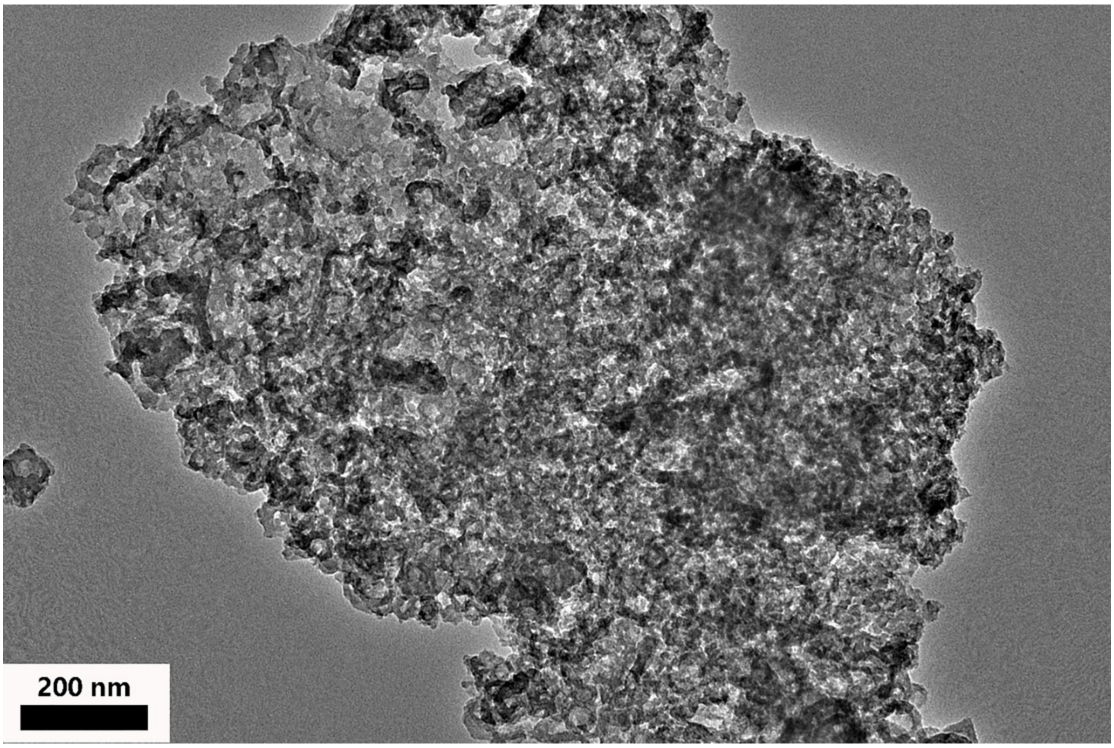

Figure S6. TEM image of PLA_{150}-PS_{250}-N_4 precursors by directly pyrolysed at 900 ^{o}C without any pre-carbonization process under heating rate of 5 ^{o}C.

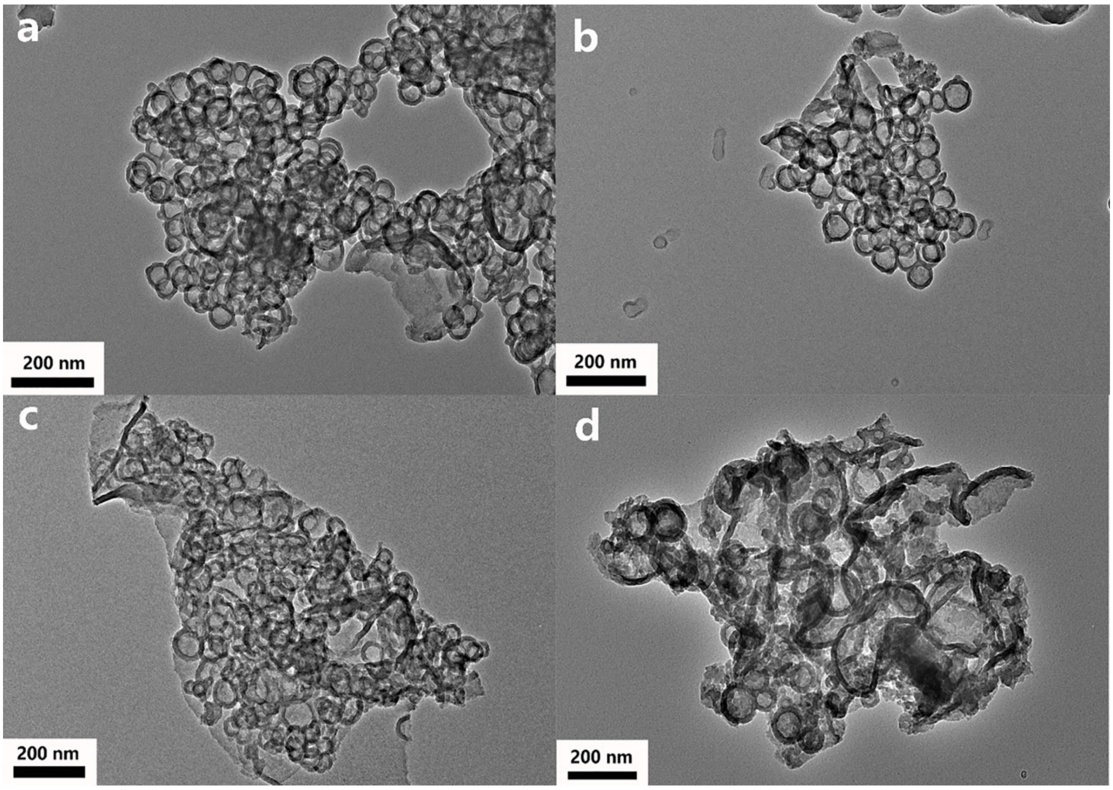

Figure S7. TEM of (a) PLA_{150}-PS_{250}-N_4-700-10H; (b) PLA_{150}-PS_{250}-N_4-800-10H; (c) PLA_{150}-PS_{250}-N_4-900-5H; (d) PLA_{150}-PS_{250}-N_4-900-20H.

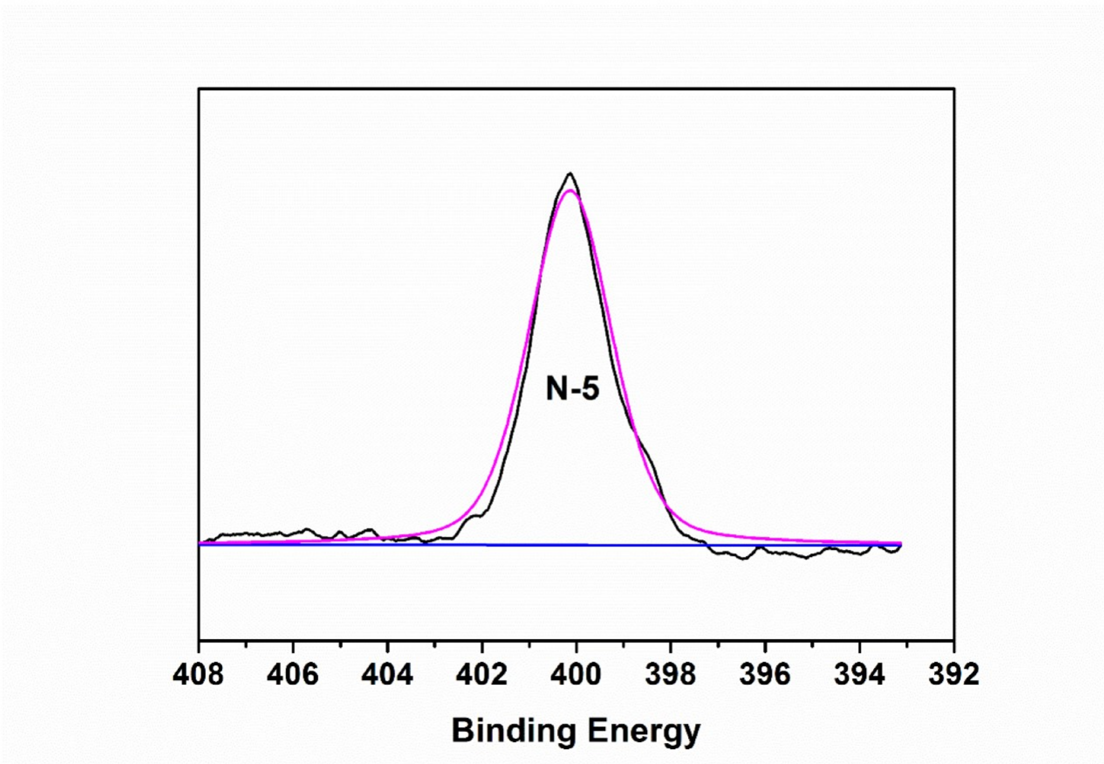

Figure S8. N 1S spectra of PLA_{150}-PS_{250}-N_4.

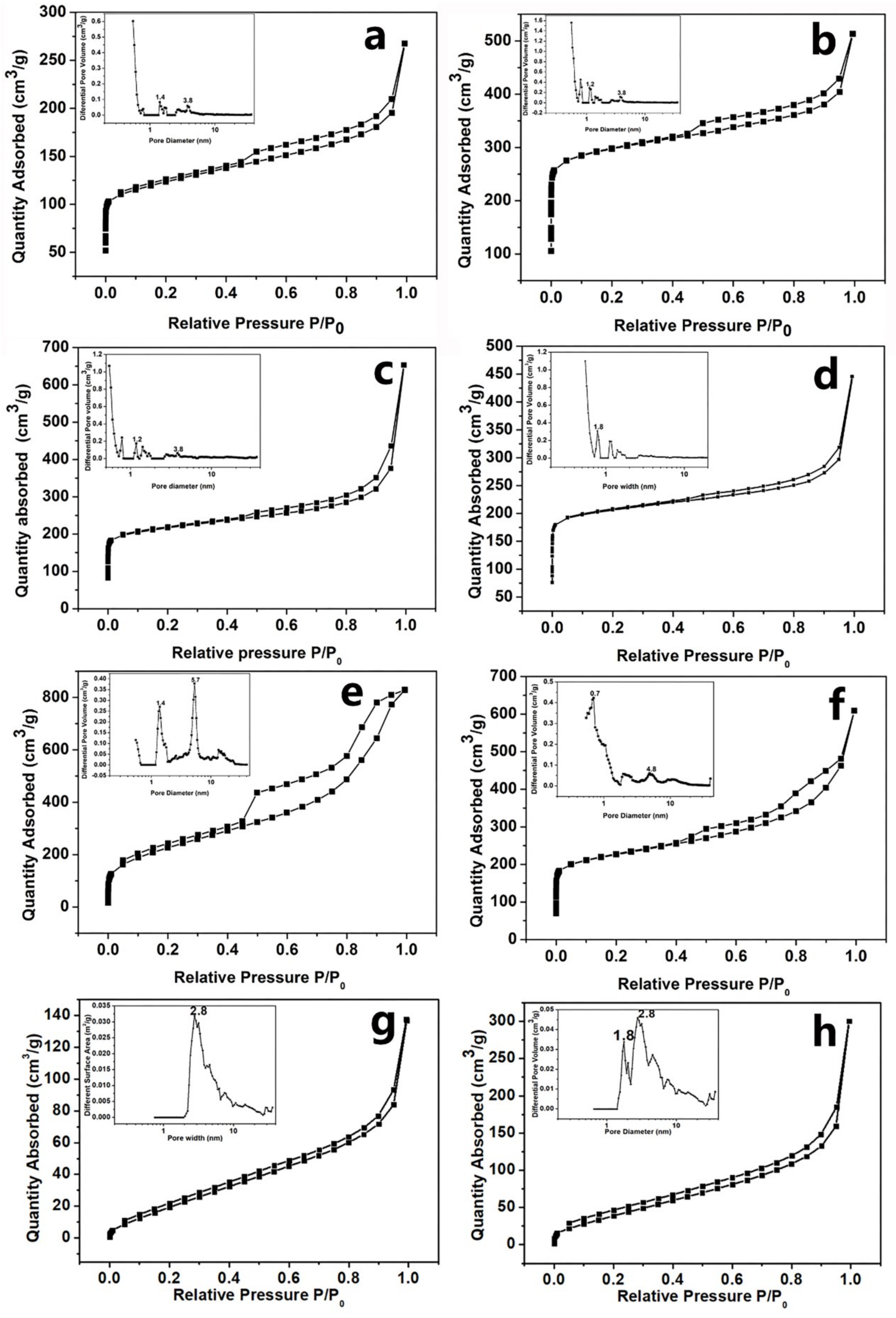

Figure S9. BET of (a) PLA_{150}-PS_{250}-N_4-700-10H; (b) PLA_{150}-PS_{250}-N_4-800-10H; (c) PLA_{70}-PS_{100}-N_4-900-10H; (d) PS_{250}-N_4-900-10H; (e) PLA_{150}-PS_{250}; (f) PLA_{150}-PS_{250}-900-10H; (g) PLA_{150}-PS_{250}-N_4; (h) PS_{250}-N_4.

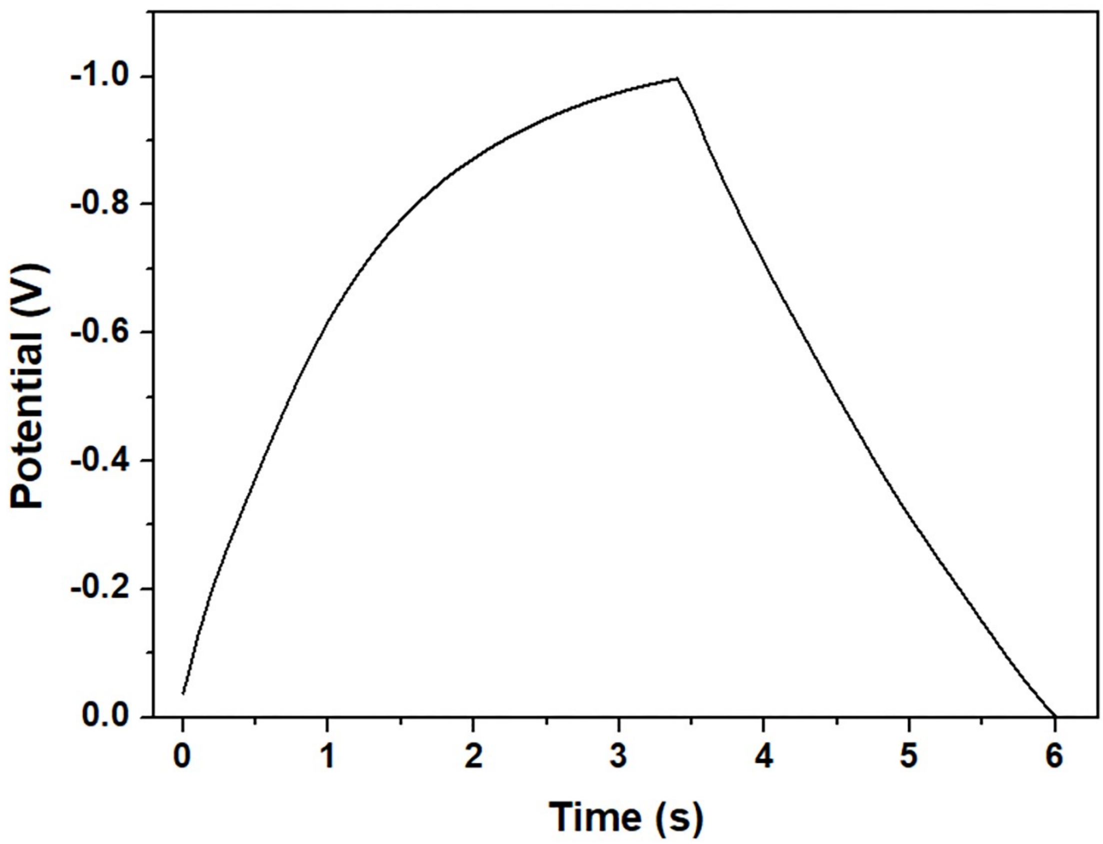

Figure S10. Galvanostatic charge-discharge curve under density of 1.0 A g^{-1}.

Table S1. Relative contents of various N configurations in samples at different calcination temperatures.

Calcination temperature (℃)	Pyridinic N (N-6) (%)	Pyrrolic N (N-5) (%)	Graphitic N (N-Q) (%)
700	25	54	21
800	23	50	27
900	13	24	63

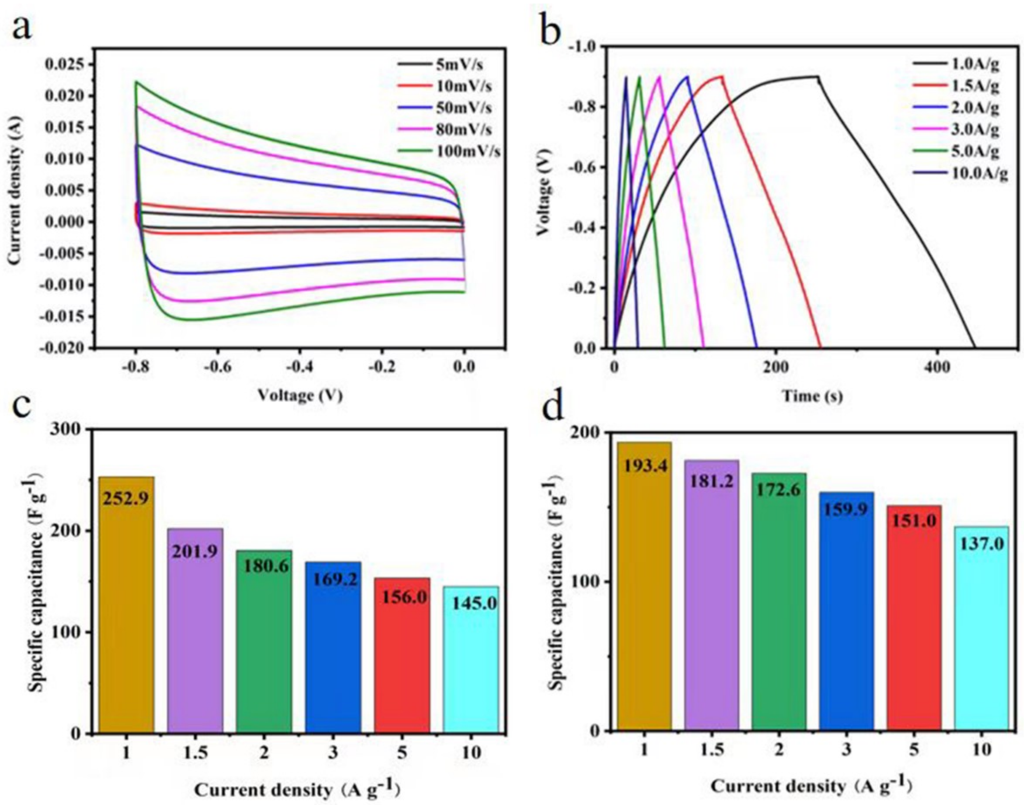

Figure S11. The dual-electrode system electrochemical test of PLA_{150}-PS_{250}-N_4-900-10H. (a) CV curves at different sweep rates; (b) galvanostatic charge-discharge curves under various current densities; (c) charge specific capacitance at different current densities; (d) discharge specific capacitance at different current densities.

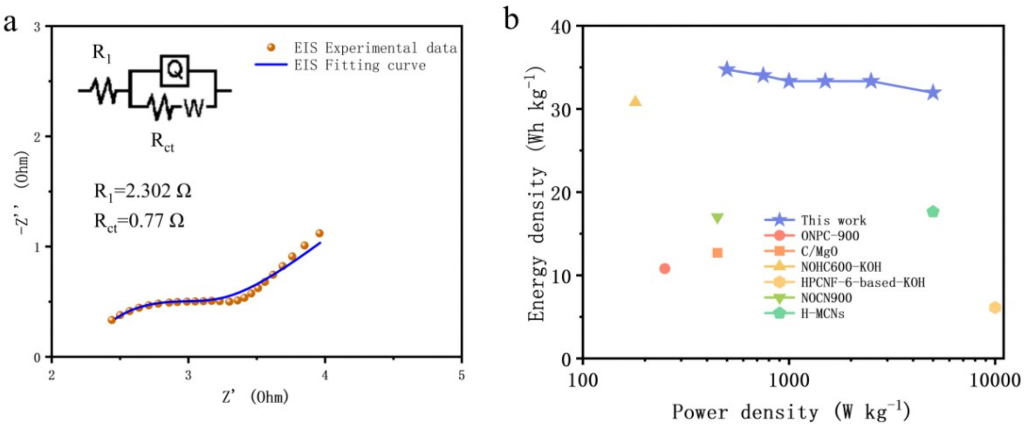

Figure S12. The three-electrode system electrochemical test of PLA_{150}-PS_{250}-N_4-900-10H. (a) electrochemical impedance spectra; (b) comparison of energy density ragone plots.

Table S2. Comparison of electrochemical performance of various carbon materials.

Sample	N content (%)	Specific capacitance (F g^{-1})	Cycling	Ref.
NHCSs	7.2	122 (0.5 A/g)	94% (1000)	1
PNHCS	6.7	213 (0.5 A/g)	91% (5000)	2
NPC900	2.2	230 (0.5 A/g)	~98% (1500)	3
NONCs	4.5	186 (0.5 A/g)	93% (5000)	4
N-OMC	11.6	216 (0.1 A/g)	100% (10000)	5
HCNs	2.6	203 (0.1 A/g)	~98% (5000)	6
N-CNFs-900	7.2	202 (1.0 A/g)	97% (3000)	7
N-S-CNF-700	4.4	220 (0.1 A/g)	~90% (1000)	8
N-OMCS	5.3	288 (0.1 A/g)	~98% (25000)	9
HCNs	0	203 (0.1 A/g)	98% (5000)	10
CMCF	3.2	218 (1.0 A/g)	94.7% (20000)	11
CPC-FeZn	0	256 (0.1 A/g)	94% (5000)	12
$CHN_{0.5}$-700	0	189 (0.1 A/g)	94.9% (10000)	13
HPC-5	0	359 (0.5 A/g)	92% (10000)	14
HPCNF-6	1.2	343 (0.5 A/g)	92% (10000)	15
N-HPCNSs	**3.57**	**250 (1.0 A/g)**	**~98% (5000)**	**This work**

1 L. Liu, S. D. Xu, Q. Yu, F. Y. Wang, H. L. Zhu, R. L. Zhang and X. Liu, Nitrogen-doped hollow carbon spheres with a wrinkled surface: their one-pot carbonization synthesis and supercapacitor properties, Chem. Commun., 2016, 52(44), 11693–11696.

2 J. P. Han, G. Y. Xu, B. Ding, J. Pan, H. Dou and D. R. MacFarlane, Porous nitrogen-doped hollow carbon spheres derived from polyaniline for high performance supercapacitors, J. Mater. Chem. A, 2014, 2(13), 5352–5357.

3 X. H. Liu, L. Zhou, Y. Q. Zhao, L. Bian, X. T. Feng and Q. S. Pu, Hollow, spherical nitrogen-rich porous carbon shells obtained from a porous organic framework for the supercapacitor, ACS Appl. Mater. Interfaces, 2013, 5(19), 10280–10287.

4 Y. R. Liang, H. Liu, Z. H. Li, R. W. Fu and D. C. Wu, In situ polydopamine coating-directed synthesis of nitrogen-doped ordered nanoporous carbons with superior performance in supercapacitors, J. Mater. Chem. A, 2013, 1(45), 15207–15211.

5 H. Chen, M. Zhou, Z. Wang, S. Y. Zhao and S. Y. Guan, Rich nitrogen-doped ordered mesoporous phenolic resin-based carbon for supercapacitors, Electrochim. Acta, 2014, 148, 187–194.

6 F. Xu, Z. W. Tang, S. Q. Huang, L. Y. Chen, Y. R. Liang, W. C. Mai, H. Zhong, R. W. Fu and D. C. Wu, Facile synthesis of ultrahigh-surface-area hollow carbon nanospheres for enhanced adsorption and energy storage, Nat. Commun., 2015, 6(1), 7221.

7 L. F. Chen, X. D. Zhang, H. W. Liang, M. G. Kong, Q. F. Guan, P. Chen, Z. Y. Wu and S. H. Yu, Synthesis of nitrogen-doped porous carbon nanofibers as an efficient electrode material for supercapacitors, ACS Nano, 2012, 6(8), 7092–7102.

8 Z. Y. Wu, H. W. Liang, C. Li, B. C. Hu, X. X. Xu, Q. Wang, J. F. Chen and S. H. Yu, Dyeing bacterial cellulose pellicles for energetic heteroatom doped carbon nanofiber aerogels, Nano Res., 2014, 7(12), 1861–1872.

9 J. G. Wang, H. Z. Liu, H. H. Sun, W. Hua, H. W. Wang, X. R. Liu, B. Q. Wei and B. Wei, One-pot synthesis of nitrogen-doped ordered mesoporous carbon spheres for high-rate and long-cycle life supercapacitors, Carbon, 2018, 127, 85–92.

10 S. Feng, K. Li, P. Hu, C. Cai, J. Liu, X. Li, L. Zhou, L. Mai, B.-L. Su and Y. Liu, Solvent-Free Synthesis of Hollow Carbon Nanostructures for Efficient Sodium Storage, ACS Nano, 2023, 17(24), 23152–23159.

11 X. Li, C. Cai, L. Zhou, L. Mai and H. J. Fan, Unraveling the Capacitive Behaviors in Nanoconfined Ionophilic Carbon Pores, Advanced Materials, 2024, 36(34), 2404393.

12 J. Zhang, R. Zhang, S. Zhang, R. Gao, Q. Yang, D. Kong, B. Luo and Z. Xiao, Integrating optimized pore structure and enriched carbonyl groups into functional carbon nanomaterials for high-performance zinc-ion capacitors, Chinese Chemical Letters, 2025, 111867.

13 R. Su, T. Xue, Z. Wei, H. Hu, Y. Mu, J. Guan, R. Yin, Y. Yi, L. Zang, C. Yang and L. Zeng, Machine learning-assisted prediction and design of biomass-derived N-doped porous carbon for zinc-ion hybrid

capacitors, Chinese Chemical Letters, 2025, 111954.
14 X. Jiao, H. Liu, X. Wei, B. Yang and B. Chang, Nano-MgO Templated Three-Dimensional Hierarchically Porous Carbon Nanosheets with Tunable Porosity for High-Rate Supercapacitors, ACS Applied Energy Materials, 2025, 8(19), 15282–15291.
15 W. Shi, Z. Zhao, A. Jiang, Y. Ma, Y. Yan, B. Yang and B. Chang, Ball-flower-like hierarchically porous carbons via a “work-in-tandem” strategy for effective energy storage and CO_2 capture, Journal of Energy Storage, 2024, 84, 110636.